DFT energy stability of group 1–group 13 hydrides for hydrogen storage applications

Yannick Elst
Faculty of Science, Free university of Brussels *

Vojtěch Laitl
Faculty of Science, University of Antwerp †

Garima Monga
Department of Chemistry, Indian institute of Technology, Roorkee ‡

Simon Vandersnickt
Faculty of Science, Ghent University §
(Dated: December 5, 2023)

This paper involves computational formation energy screening of selected group 1–group 13 ternary hydrides potentially relevant for hydrogen storage applications. Crystalline structure data of the NaH–AlH_3 diagram are reviewed and analogous structures thereof are sought for in KH–AlH_3 and Na–GaH_3 phases. A few of the latter structures are calculated for the first time reported, and although we did not find a decisive H_2 storage candidate in among their ground states, outlook remarks are still given for both experiment and computation.

Keywords: hydrogen storage — ternary hydrides — density functional theory — energy stability

I. INTRODUCTION

Recent years of industry electrification and ongoing transition to fossil fuel-free society have paved the way for excessive research within the topic of hydrogen-based fuels. Given, however, the intrinsic volume demands of hydrogen gas, concerns are risen about its safe and efficient storage and transfer. Looking for suitable hydrogen storage materials is therefore vital in this fuel technology.

A well-known hydrogen storing method is exemplified by interstitial noble metal hydrides [1]. In such phases, H_2 is reversibly bound by increased pressure, which comes along with an order-of-magnitude lowering of storage volumes. However, due to their cost inefficiency, noble metals do not represent a large-scale solution, and attempts have thus been made to employ materials based on accessible ionic or covalent hydrides. [2] gives an overview of H_2 release mechanisms pertaining to several such compounds, including, *e.g.*, LiH, AlH_3, or $NaAlH_4$. Besides the typical thermal dehydrogenation outlined therein, we remark that strictly controlled chemical leaching, for instance of the form

$$\mathrm{NaAlH_4} + 4\,\mathrm{H_3O^+} \longrightarrow \mathrm{Na^+} + \mathrm{Al^{3+}} + 4\uparrow\mathrm{H_2} + 4\,\mathrm{H_2O},$$

may represent a hydrogen release mechanism as well. With that in regard, hydrogen-rich complex hydrides become an interesting class of storage compounds, albeit at a possible cost of their larger crystalline phase volumes.

As an illustrative example, [3] briefly envisages the role of Na_3AlH_6 in the hydrogen storage applications of $NaAlH_4$. This work is inspired by such findings and computationally explores the energy stability of Na–Al–H crystalline phases rich in hydrogen. To further exemplify our results, we also hypothesise on the occurrence of similar structures in K–Al–H and Na–Ga–H phases.

II. METHODS

This study entails a computational screening of crystalline phases energy stability performed in the DFT framework of Quantum Espresso [4, 5]. The screening was benchmarked by the NaH–AlH_3 phase diagram whose ground-state members were retrieved from the Materials Project database [6]. Key properties of their primitive unit cells are shown in Tab. I. The "H_2 content" is expressed as the number of net H_2 pairs per unit cell volume, and this is converted onto a hypothetical ideal gas pressure at room temperature (*cf.* Appendix A). "Atoms" and "DOF" are the total number of atoms and geometrical degrees of freedom fully characterising each cell.

TABLE I. Primitive cell properties of NaH–AlH_3 phase diagram members.

	Atoms	DOF	H_2 content (Å^{-3})	p_{H_2} (MPa)
AlH_3 ($Fd\bar{3}m$) [7]	16	2	3.3×10^{-2}	134
$NaAlH_4$ ($I4_1/a$) [8]	12	14	3.0×10^{-2}	121
Na_3AlH_6 ($P2_1/c$) [9]	20	5	2.7×10^{-2}	110
$Na_5Al_3H_{14}$ ($P4/mnc$) [10]	44	10	3.1×10^{-2}	125
NaH ($Fm\bar{3}m$) [11]	2	1	1.8×10^{-2}	74

Perdew–Burke–Ernzerhof (PBE) exchange correlation

* Yannick.Elst@vub.be
† vojtech.laitl@student.uantwerpen.be
‡ garima@cy.iitr.ac.in
§ simon.vandersnickt@ugent.be

functional is employed with the kinetic energy cutoffs of 75 Ry and 375 Ry respectively for wavefunctions and charge density. A typical k–mesh size of $6\times6\times6$ was applied in case of cubic crystals; extensions to more general geometries are shown in Appendix A, alongside with a typical convergence test. Pseudopotential-defined basis was used for the computation, and PBE pseudopotentials were adopted per element from [12].

Full geometrical optimisation ('vc–relax') employing the Broyden–Fletcher–Goldfarb–Shanno (BFGS) algorithm of damped Newtonian nuclei dynamics (*cf.* [4, 5] herein) was later employed to assess the ground state energy of Tab. I's compounds and thus to locate their position in a phase diagram.

Finally, an attempt was made to improve such properties by trial optimisation of respectively the group 1 cation and group 13 central atom of $NaAlH_4$-like ternary hydrides. For simplicity in such screenings, we limit ourselves to 0 K (*i.e.*, ground state) calculations.

III. RESULTS AND DISCUSSION

Fig. 1 depicts the predicted formation energies in a phase diagram, following a standard normalisation procedure exemplified in Appendix A. Negligible (≤ 0.4 %) differences are observed between the Materials Project data and the results of our optimisation, suggesting that the former are very close to ground state energies and structures of all such phases. Moreover, all phases involved lie on convex hull(-like) trend lines, rendering them stable against decomposition into any other. That is in good agreement with Tab. I's references which mark $NaAlH_4$ stable and the other hydrides as stable products of its decomposition at elevated temperatures.

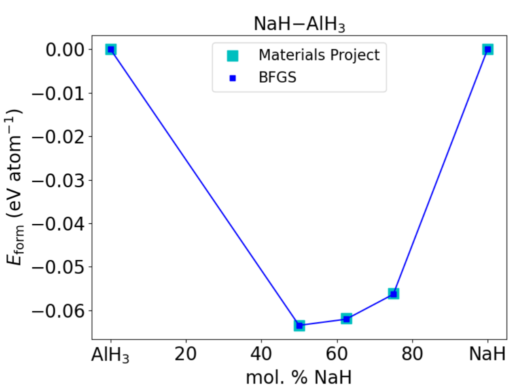

FIG. 1. Ground state NaH–AlH_3 phase diagram.

$NaAlH_4$ is also indicated as the most stable ground state phase. Comparing the formation energies with hydrogen storage capacities, however, marks $Na_5Al_3H_{14}$, too, as an interesting H_2 storage candidate of similar characteristics. Since [10] solely describes its theoretical structure, further experimental work may be inspired by our observations.

As a follow-up, structures of $XAlH_4$, X=Li, K, Rb, and $NaYH_4$, Y=B, Ga, were retrieved from [6] and screened for H_2 storage capacity and formation energies as analogues of $NaAlH_4$. Following indicative results of Appendix B, KH–AlH_3 and NaH–GaH_3 phases were chosen as viable candidates. An elaborate study of possible counter choices can be found elsewhere [13].

Among KH–AlH_3 phases, $K_5Al_3H_{14}$ has not been analysed by records available to the authors. As an indicative, we predicted its energy by assuming $K_5Al_3H_{14}$ isostructural to $Na_5Al_3H_{14}$ and using the lattice parameter of $a(K_5Al_3H_{14}) = a(KAlH_4)/a(NaAlH_4)$ as a first BFGS guess. Final results are shown in Fig. 2.

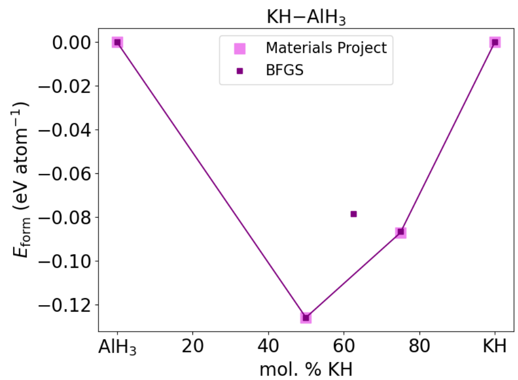

FIG. 2. Ground state KH–AlH_3 phase diagram. $K_5Al_3H_{14}$ (62.5 mol. % KH) is predicted by this work.

Although a reasonable enhancement of formation energies is generally indicated, only the structures already known to [6] are now predicted as stable at 0 K. The same is observed in case of NaH–GaH_3 phases in Fig. 3. Here, although Na_3GaH_6 stoichiometries were experimentally observed [14], no definite structural determination has been known to the authors for Na_3GaH_6 or $Na_5Ga_3H_{14}$.

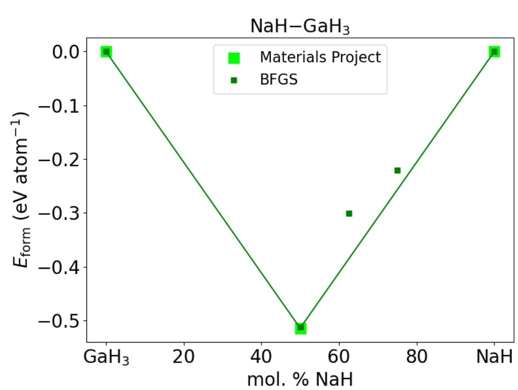

FIG. 3. Ground state NaH–GaH_3 phase diagram. Na_3GaH_6 (75.0 mol. % NaH) and $Na_5Ga_3H_{14}$ (62.5 mol. % NaH) are predicted by this work.

First guesses to the structure of Na_3GaH_6 and $Na_5Ga_3H_{14}$ were obtained within the same rationale as that of $K_5Na_3H_{14}$. Although neither of such crystals is found stable against decomposing into NaH and $NaGaH_4$, we note that the structure estimates may only be ballpark ones. In the particular case of $Na_5Ga_3H_{14}$, numerical instabilities were encountered in estimating the BFGS's optimum electronic properties, suggesting that the real ground state structure might lie elsewhere. Moreover, in the NaH–GaH_3 case, the vicinity of higher hydrides to the convex hull may still find them interesting for elevated temperature crystallisation protocols.

Finally, the properties of Fig. 2–3's phases are summarised as follows in Tab. II. Drawing upon similar formation energy–storage capacity arguments as for NaH–AlH_3, $KAlH_4$ and $NaGaH_4$ are marked as ternary structures potentially interesting for experimental hydrogen storage. For Ga phases, an improvement (+63 or +67 MPa) is observed over the Na candidates (respectively $NaAlH_4$ or $Na_5Al_3H_{14}$), while for K, the storage capacity is remarkably worsened (−37 or −41 MPa).

TABLE II. Hydrogen storage properties of Fig. 2–3's phases.

	Atoms	H_2 content (Å^{-3})	p_{H_2} (MPa)
KH (Fm$\bar{3}$m) [15]	2	1.1×10^{-2}	42
$KAlH_4$ (Pnma) [16]	24	2.2×10^{-2}	84
K_3AlH_6 (P2_1/c) [17]	20	2.0×10^{-2}	82
$K_5Al_3H_{14}$ (P4/mnc)^a	44	2.3×10^{-2}	95
GaH_3 (I4/mmm) [6]	4	1.1×10^{-1}	431
$NaGaH_4$ (Cmcm) [18]	12	4.9×10^{-2}	188
Na_3GaH_6 (P2_1/c)^a	20	2.5×10^{-2}	97
$Na_5Ga_3H_{14}$ (P4/mnc)^a	44	2.8×10^{-2}	107

a this work

IV. CONCLUSIONS AND OUTLOOK

This study comprises DFT-level energy stability screening of $NaAlH_4$-like crystalline phases for potential hydrogen storage applications. $NaAlH_4$ itself and theoretical $Na_5Al_3H_{14}$ were marked as viable candidates, and their analogues were sought for in analogous KH–AlH_3 and NaH–GaH_3 0 K phase diagrams. Although almost an order-of-magnitude formation energy enhancement was observed *en route* from NaH–AlH_3 to NaH–GaH_3 phases, neither of the newly calculated structures were denoted as stable ground state phases.

We have remarked, however, that such findings themselves do not disregard the newly screened structures from further computational (*e.g.*, electronic structure description) or/and experimental (*e.g.*, finite temperature crystallisation protocols) studies. Such or related work is therefore a possible outlook to this study.

ACKNOWLEDGMENTS

Stefaan Cottenier, Ph.D., (UGent) is warmly thanked for providing complete professional guidance and support to the authors in the framework of a Computational Materials Physics course.

Appendix A: Data preparation and postprocessing

Fig. **A**I exemplifies the convergence settings results shown for the pressure tensor of $NaAlH_4$. Each of the subsequent panels takes as a settings input the parameter(s) optimised above, and the thresholds marked in the main text are clearly seen.

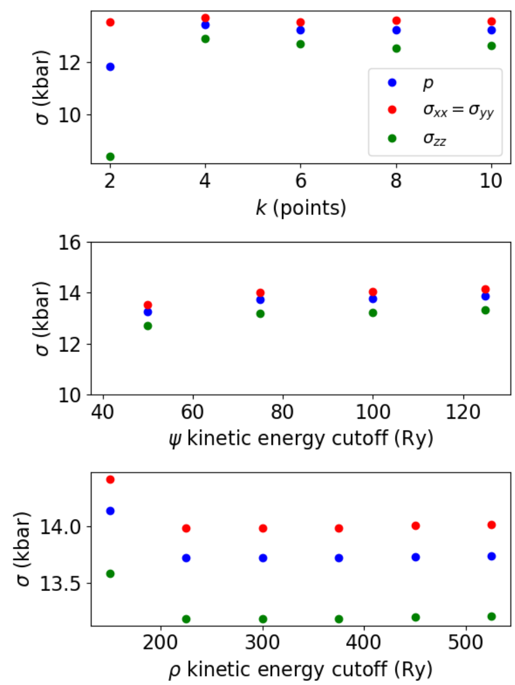

FIG. **A**I. $NaAlH_4$ stress tensor convergence settings.

For the $NaAlH_4$ noncubic cell of $a : b : c \doteq 1 : 1 : 2$ lattice parameters, the full k–mesh is of the size $6 \times 6 \times 3$, rather than the cubic $6 \times 6 \times 6$. This or similar scaling was followed for all noncubic cells involved (*cf.* Tab. I–II for space groups).

$NaAlH_4$'s full primitive cell stoichiometry reads $Na_2Al_2H_8$ (see Tab. I). With its volume of 134.15 Å^3, this translates to H_2 content of $4/134.15 \doteq 3.0 \times 10^{-2}$ Å^{-3} and hence to $p_{H_2} \doteq 3.0 \times 10^{-2} \times 10^{30} \cdot 293 k_B \doteq 121 \times 10^6$ Pa at 293 K. Similar computations are employed for all structures in the main text.

Key for data postprocessing was the conversion of total DFT energies into the formation energies. This is done by assuming the stoichiometry of a ternary phase as compared to its binary end members. For NaH–AlH_3, this reads

$$\frac{1}{2}\,\mathrm{Al_4H_{12}} + 2\,\mathrm{NaH} \longrightarrow \mathrm{Na_2Al_2H_8}$$
$$\frac{1}{2}\,\mathrm{Al_4H_{12}} + 6\,\mathrm{NaH} \longrightarrow \mathrm{Na_6Al_2H_{12}}$$
$$\frac{3}{2}\,\mathrm{Al_4H_{12}} + 10\,\mathrm{NaH} \longrightarrow \mathrm{Na_{10}Al_6H_{28}}$$

where the full primitive cell stoichiometry is included. The formation energy is then read as the reaction energy of the above hypothetical equations and normalised onto the total number of right-hand side atoms. By convention, binary hydrides are ascribed 0 eV/atom each. All other phase diagrams are assembled correspondingly.

Appendix B: Supplementary data

Original data underlying this study are available on-line *via* an external repository (https://shorturl.at/zJLQ3). To support the main text, we extract below the results of our $XAlH_4$ and $NaYH_4$ screening, as calculated based on [6]'s ground state structures.

TABLE **A**I. Indicative results of X, Y screening

Structure	Formation energy (eV/atom)	p_{H_2} (MPa)
$XAlH_4$, X=Li, K, Rb		
$LiAlH_4$	~ 0	110
$KAlH_4$	-0.13	84
$RbAlH_4$	-0.15	75
$NaYH_4$, Y=B, Ga		
$NaBH_4$	-0.24	143
$NaGaH_4$	-0.51	188

The formation energies were approximated by omitting the optimisation step from the main text's protocol.

[1] G. Gao, H. Wang, L. Zhu, and Y. Ma, Pressure-induced formation of noble metal hydrides, Journal of Physical Chemistry C **116**, 1995 (2012).

[2] Y. Luo, Q. Wang, J. Li, F. Xu, L. Sun, Y. Zou, H. Chu, B. Li, and K. Zhang, Enhanced hydrogen storage/sensing of metal hydrides by nanomodification, Materials Today Nano **9**, 10.1016/j.mtnano.2019.100071 (2020).

[3] M. Fichtner, J. Engel, O. Fuhr, O. Kircher, and O. Rubner, Nanocrystalline aluminium hydrides for hydrogen storage, Materials Science and Engineering: B **108**, 42 (2004).

[4] P. Giannozzi, S. Baroni, N. Bonini, M. Calandra, R. Car, C. Cavazzoni, D. Ceresoli, G. L. Chiarotti, M. Cococcioni, I. Dabo, *et al.*, QUANTUM ESPRESSO: a modular and open-source software project for quantum simulations of materials, Journal of physics: Condensed matter **21**, 395502 (2009).

[5] P. Giannozzi, O. Andreussi, T. Brumme, O. Bunau, M. B. Nardelli, M. Calandra, R. Car, C. Cavazzoni, D. Ceresoli, M. Cococcioni, *et al.*, Advanced capabilities for materials modelling with QUANTUM ESPRESSO, Journal of physics: Condensed matter **29**, 465901 (2017).

[6] A. Jain, S. P. Ong, G. Hautier, W. Chen, W. D. Richards, S. Dacek, S. Cholia, D. Gunter, D. Skinner, G. Ceder, *et al.*, Commentary: The materials project: A materials genome approach to accelerating materials innovation, APL materials **1** (2013).

[7] P. Vajeeston, P. Ravindran, and H. Fjellvåg, Stability enhancement by particle size reduction in AlH_3, Journal of alloys and compounds **509**, S662 (2011).

[8] T. J. Frankcombe and O. M. Løvvik, The crystal structure and surface energy of $NaAlH_4$: A comparison of DFT methodologies, The Journal of Physical Chemistry B **110**, 622 (2006).

[9] E. Rönnebro, D. Noréus, K. Kadir, A. Reiser, and B. Bogdanovic, Investigation of the perovskite related structures of $NaMgH_3$, $NaMgF_3$ and Na_3AlH_6, Journal of alloys and compounds **299**, 101 (2000).

[10] J. G. Ojwang, R. van Santen, G. J. Kramer, and X. Ke, An ab initio study of possible pathways in the thermal decomposition of $NaAlH_4$, Journal of Solid State Chemistry **181**, 3037 (2008).

[11] J. H. Lei, Z. Z. Yan, H. Duan, and Y. J. Zhang, Theoretical study on crystal structure and hydrogen storage properties of sodium hydride, Advanced Materials Research **287**, 1348 (2011).

[12] G. Prandini, A. Marrazzo, I. E. Castelli, N. Mounet, and N. Marzari, Precision and efficiency in solid-state pseudopotential calculations, npj Computational Materials **4**, 72 (2018), http://materialscloud.org/sssp.

[13] T. Ghellab, Z. Charifi, H. Baaziz, Uğur, G. Uğur, and F. Soyalp, First principles study of hydrogen storage material $NaBH_4$ and $LiAlH_4$ compounds: Electronic structure and optical properties, Physica Scripta **91**, 10.1088/0031-8949/91/4/045804 (2016).

[14] T. N. Dymova and Y. M. Dergachev, Reaction of alkali metals with gallium, Inorganic Chemistry , 1193 (1981).

[15] V. Kuznetsov and M. Shkrabkina, X-ray diffraction study of NaH and KH at temperatures from 20 to 400 °c, Journal of Structural Chemistry **3**, 532 (1962).

[16] P. Vajeeston, P. Ravindran, A. Kjekshus, and H. Fjellvåg, Crystal structure of $KAlH_4$ from first principle calculations, Journal of alloys and compounds **363**, L8 (2004).

[17] P. Vajeeston, P. Ravindran, A. Kjekshus, and H. Fjellvåg, First-principles investigations of aluminum hydrides: M_3AlH_6 (M = Na, K), Physical Review B **71**, 092103 (2005).

[18] Y. Z. Nozik, E. Kuklina, N. Bliznyuk, and S. Borisov, Crystal structure of sodium tetrahydro (deutero) gallate (T= 80 K), Soviet Physics-Crystallography (English Translation) **36**, 29 (1991).